Chemical and Process Engineering Research
ISSN 2224-7467 (Paper) ISSN 2225-0913 (Online)
Vol.65, 2023

The Optical Qualities of a Solution Made of Copper-doped Silver Sulfide Colloidal Nanoparticles

Nasser K. Hejazy
Technology & Applied Sciences, Al-Quds Open University, Gaza GFM3+FPW, Gaza Strip, Palestine
E-mail of the corresponding author: nkhejazy@hotmail.com

Abstract
The researchers present new optical properties of Cu-doped Ag_2S colloidal solution synthesized via a wet chemical method. They investigate the effects of doping on nanoparticle properties. TEM images reveal spherical samples with sizes ranging from 6 to 18 nm. Doped samples exhibit a redshift in absorption spectra compared to pure Ag_2S. Additionally, Pl intensity decreases with increasing Cu concentration. Size estimation from absorption spectra aligns with TEM results, with slight variations. This study unveils the unique optical characteristics of Cu-doped Ag_2S colloidal solution, shedding light on the impact of doping and providing valuable insights into nanoparticle behavior and synthesis techniques.
Keywords: Metal (Cu); Doped- Ag_2S; Optica; Photoluminescence
DOI: 10.7176/CPER/65-04
Publication date: November 30th 2023

1. Introduction

The optical properties of semiconductor nanostructures are significantly influenced by their shape, size, and composition [1-6]. These nanomaterials exhibit distinct characteristics attributed to quantum-size effects, stemming from their increased surface atoms [7,8]. Transition metal chalcogenides are particularly important in nanotechnology due to their remarkable photoelectronic properties, finding applications in diverse fields such as solar cells, sensors, computers, and medicine [9]. Among these chalcogenides, Ag_2S stands out with its direct bandgap (0.9-1.05 eV), exceptional absorption, optical limiting capabilities, and chemical stability [15,16]. Various techniques, including microemulsions, sol-gel methods, ion implantation, sonochemical processes, gamma-irradiation, and organic-metallic precursors, are employed for the synthesis of Ag_2S nanoparticles [17-22]. Doping semiconductor nanocrystals with metals offers new possibilities for illumination by creating additional electronic levels within bandgaps and modifying the band structure [23].

Previous studies have focused on investigating the optical properties of Cd-doped and Co-doped Ag_2S nanoparticles. Notably, Ali Fakhri et al. [24] synthesized Cu-doped Ag_2S nanoparticles using a straightforward chemical co-precipitation method. High-resolution transmission electron microscopy (TEM) analysis confirmed their spherical morphology, with an average diameter of 30 nm. Photoluminescence (Pl) measurements revealed a shift in the emission wavelength, ranging approximately from 456 to 477 nm. Another investigation conducted by E.S. Aazam involved the preparation of Ni-doped Ag_2S nanoparticles using a hydrothermal method. The study explored the influence of Ni dopants on the photocatalytic activity of Ag_2S [25].

2. Experimental

2.1 Synthesis

High-quality chemicals, including silver sulfate (Ag_2S), copper sulfate ($CuSO_4.8H_2O$), and sodium sulfide ($Na_2S.xH_2O$), were sourced from Merck and used as precursors. Analytical reagent grade reagents were utilized without purification, while all glassware underwent acid washing. Dilutions and sample preparations were conducted using distilled water. In the preparation of pure Ag_2S colloidal solution, a wet chemical method was employed. Firstly, 0.1 mmol of $AgNO_3$ was dissolved in 50 ml of distilled water. The resulting solution was then slowly added dropwise to 50 ml of 0.1 M Na_2S solution while stirring until a transparent pale-yellow solution was achieved.

For the preparation of Cd and Co-doped Ag_2S colloidal solutions, a mixture solution comprising 25 ml of 0.001 M Ag_2SO_4, 25 ml of 0.001 M $CuSO_4.8H_2O$, and 25 ml of 0.001 M Na_2S aqueous solution was prepared. Subsequently, 25 ml of a 0.001 M Na_2S solution was added dropwise to the mixture solution while stirring, until a transparent clear solution was achieved. The colors of the resulting solutions varied depending on the dopant type and amount. These synthesized colloidal solutions of Ag_2S nanoparticles were utilized for all subsequent measurements and analyses.

2.2 Instrumentation

UV-vis absorption spectra (200-700 nm) were collected using a Shimadzu UV-2400 spectrophotometer. PL spectra were obtained with a JASCO FP-6500 spectrofluorometer, selecting an extinction wavelength of 350 nm for Cu-doped Ag_2S nanoparticles. TEM analysis was conducted using a JEOL JEM2010 transmission electron

microscope.

3. Results and Discussion

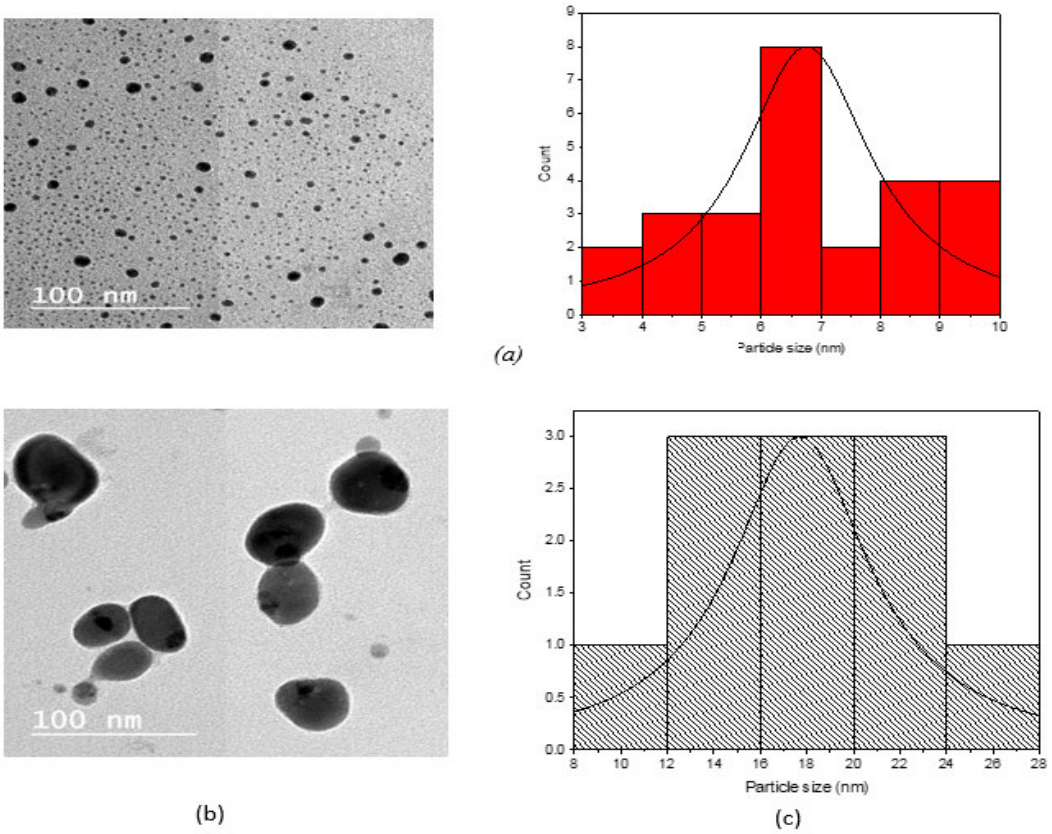

Figure 1: TEM images and histograms, a) Undoped Ag_2S, b) 6 % Cu-doped Ag_2S, and c) 6 % Cu-doped Ag_2S

Fig.1 (a-c) illustrates the morphology and histograms of undoped and 6% Cu-doped Ag_2S nanoparticles. The particles exhibited a range of shapes, varying from spherical to ellipsoid. Also,

Fig.1 (a-c) depicts histograms of pure and Cu-doped Ag_2S nanoparticles, with average individual particle sizes ranging from 6 to 18 nm.

The examination of UV-vis spectrum analysis proves to be an effective method for investigating how doping affects the optical properties of Ag_2S nanoparticles [26,27]. Figure 2 visually presents the absorption spectra of both pristine and Cu-doped Ag_2S nanoparticles.

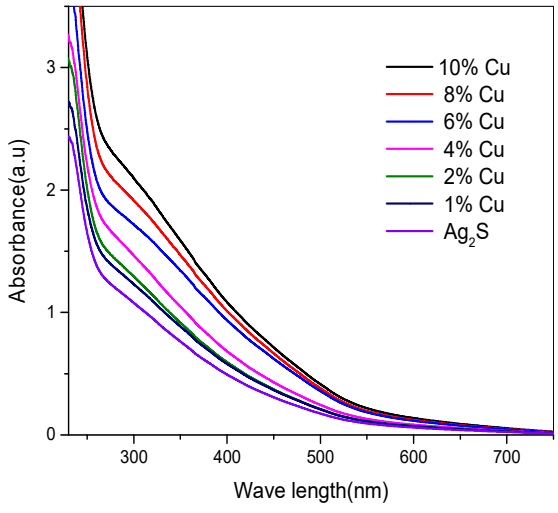

Figure 1. UV–vis spectra of Cu-doped Ag_2S nanoparticles

The UV-vis spectra exhibited a gradual rise in absorbance across the 230 nm to 800 nm range. In Fig.2, it is evident that the optical absorption edge of Ag_2S nanoparticles shifts towards longer wavelengths with an escalation in Cu concentration. The estimation of optical band gap energies for various dopants is accomplished using Tauc's relation, provided below [28].

$$(\alpha h\nu)^{\frac{1}{n}} = A(h\nu - E_g) \tag{2.3}$$

The constant A and band gap energy (Eg) of the material are related by the equation provided. By plotting (αhν)2 against hν and extrapolating the curve's straight portion on the hν axis at α = 0, the direct band gap of the samples is calculated. Fig. 3 demonstrates straight-line plots, indicating that Cu-doped Ag_2S samples possess a direct energy band gap ranging from 2.42 to 2.22 eV.

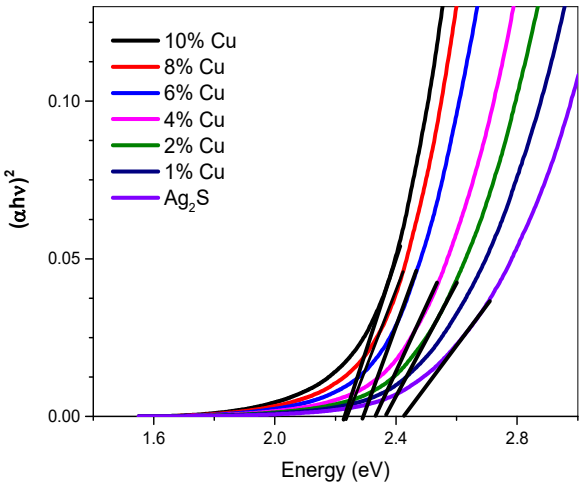

Figure 3. The band gap energy of Cu-doped Ag_2S nanoparticles

The decrease in the energy gap was evident with the rising presence of Cu ions, as depicted in Fig. 3. This phenomenon of redshift can be attributed to an increase in particle size, leading to alterations in energy levels and a slight reduction in the band gap. Similar observations were reported in the case of Cu-doped CdS [29]. To understand the size-dependent behavior of Cu-doped Ag_2S, the band gap energy can be approximated using an effective mass approach, as expressed in the following equation.

$$E_g \cong E_g^{bulk} + \frac{\hbar^2\pi^2}{2er^2}\left(\frac{1}{m_e m_0} + \frac{1}{m_h m_0}\right) - \frac{1.8e}{4\pi\varepsilon\varepsilon_0 r} \tag{2}$$

In the equation, Eg represents the bulk band gap (eV), ħ denotes Planck's constant, r signifies the particle radius, me denotes the electron effective mass, mh represents the hole effective mass, mo denotes the free electron mass, e represents the charge on the electron, ε denotes the relative permittivity, and ε0 stands for the permittivity of free space. For Ag_2S, it is commonly acknowledged that ΔEg is 1.0 eV, while me (0.22 m0) and mh (1.096 m0) denote the electron and hole effective masses, respectively [30]. The relative permittivity (ε) is 5.95 [31].

Table 1. presents the band gap values of Cu-doped Ag_2S nanoparticles synthesized with different cobalt concentrations.

Concentration	Energy gab (ev)	Particle size (nm)
0.00	2.42	6.5
0.01	2.37	6.88
0.02	2.36	8.94
0.04	2.33	10.06
0.06	2.29	12.28
0.08	2.24	14.65
0.10	2.23	16.65

Table 1 provides the band gap values of the particles synthesized with different cadmium concentrations, along with the corresponding particle sizes calculated using
equation (2)

The observed reduction in band gap energy with increasing particle size, attributable to quantum size confinement (Fig. 4), aligns with the TEM measurements. These findings emphasize the synthesis method's capacity to control the dimensions of Cu-doped Ag_2S nanoparticles and their associated optical properties.
Table 1 presents the band gap values of Cu-doped Ag_2S nanoparticles, obtained with different cobalt concentrations, along with the corresponding particle sizes calculated using equation (2). Figure 5, shown below, illustrates the relationship between band gap energy and particle size. The data clearly demonstrates a decrease in band gap energy as the particle size increases, attributable to the phenomenon of quantum size confinement. The estimation of Cu-doped Ag_2S particle size was accomplished using Brus equation, yielding results that align with the TEM analysis.

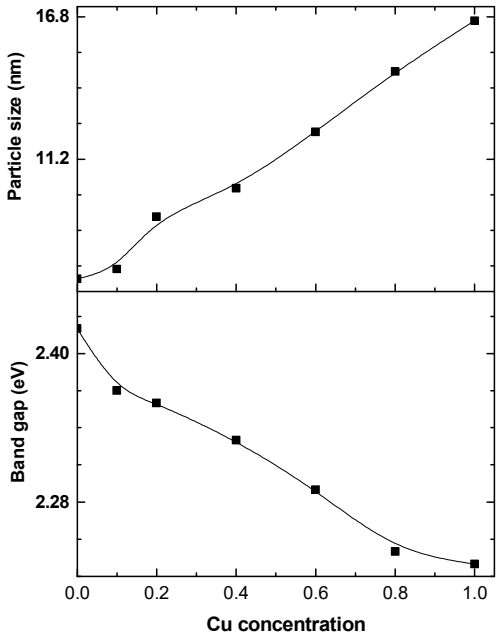

Figure 4: Variations of band gap energy with particle size of Cu-doped Ag_2S nanoparticles.

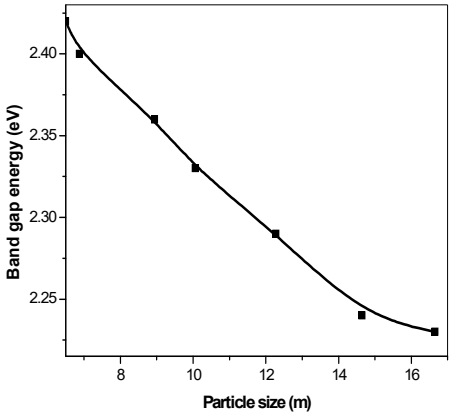

Figure 5: Variation of band gap energy with the particle size of Cu-doped Ag_2S.

To gain further insights into the optical properties, room temperature photoluminescence (PL) measurements were conducted for both pure Ag_2S and Cu-doped Ag_2S nanoparticles. Figure 6 illustrates the emission spectra of the samples, with excitation performed at 350 nm.

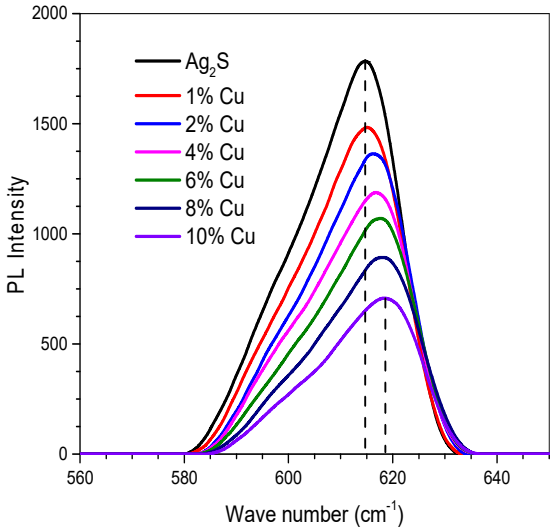

Figure 6: PL spectra of Cu-doped Ag_2S nanoparticles.

In the spectrum, notable broad emission peaks are observed at approximately 614 nm for undoped Ag_2S, 615 nm for 1% Cu-doped Ag_2S, 616 nm for 2% Cu-doped Ag_2S, 617 nm for 4% Cu-doped Ag_2S, 618 nm for 6% Cu-doped Ag_2S, 618 nm for 8% Cu-doped Ag_2S, and 618 nm for 10% Cu-doped Ag_2S. These strong visible photoluminescence (PL) peaks may be associated with crystalline defects formed during growth. Termed deep-level emissions, they arise from the recombination of photo-generated holes with electrons deeply trapped in silver interstitials and oxygen vacancies [32].

The observable decrease in photoluminescence (PL) intensity as Cu dopants increase is clear evidence. Cu acts as a trapping site, effectively capturing photogenerated electrons from the conduction band and separating electron-hole pairs. Incorporating noble metal nanoparticles into Ag_2S [33] is widely recognized to enhance visible light absorption. This enhancement leads to a redshift in the absorption edge, signifying a reduction in band gap energy. This finding is additionally corroborated by UV-vis spectra measurements.

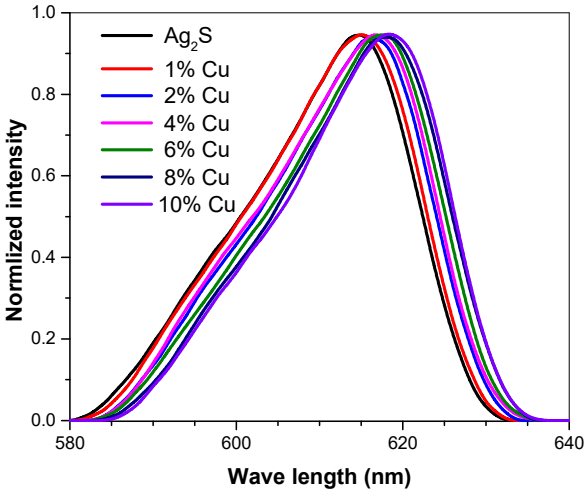

Figure 7: Normalized PL spectra of Cu-doped Ag_2S nanoparticle.

Figure 7 displays the normalized PL spectra of Ag_2S doped with varying copper concentrations of 0%, 1%, 2%, 4%, 6%, 8%, and 10%.

The introduction of Cu dopants results in a slight redshift of the emission band. This redshift is consistent with the observed expansion of particle size at higher dopant concentrations, as observed through TEM analysis. The redshift in the emission peak can be attributed to the quantum confinement effect experienced by the nanocrystals.

4. Conclusions

In our investigation, Cu-doped Ag_2S nanoparticles were successfully synthesized using a wet chemical method. TEM analysis revealed that the nanoparticles exhibited a spherical shape, with sizes ranging from 6 to 18 nm across all Cu-doped Ag_2S samples. Interestingly, an observed redshift phenomenon was found to be directly correlated with the concentration of Cu doping in Ag_2S, as evidenced by the UV-vis and PL spectra. Furthermore, as the concentration of Cu incorporated into the nanoparticles increased, the emission intensity of Cu decreased, while the intensity of red emission from Co showed an increment.

The inclusion of Cu2+ ions in Ag_2S nanoparticles leads to a unique photoluminescence (PL) phenomenon. Our experimental findings highlight the significant influence of dopants on altering the emission color of Ag_2S nanoparticles. Notably, the Brus equation used to estimate particle size consistently yields values in close agreement with those obtained from TEM analysis, particularly when quantum size confinement causes an increase in particle size.

References

Hammad, Talaat M., Kuhun, S., Abu Amsha, A., & Rolf, M., (2021), Journal of the Australian Ceramic Society, 57, 543–553.
Hammad, Talaat M., Kuhun, S., Abu Amsha, A., & Hejazy, N. K., (2020), Journal of Superconductivity and Novel Magnetism, 33, 3065–3075
Kodeh, F. S., & Hammad, T. M., (2020), Journal of Biomedical Materials Research 28, 21907-21912
Hejazy, N. K., & Hammad, T. M., (2019), Palestinian Journal of Technology & Applied Sciences - No. 2, 82-90
Hammad, T. M., Tamous, H. M., & Hejazy, N. K., (2007), International Journal of Modern Physics B 21, 4399-4406.
Hammad, T. M., (2006), International Journal of Modern Physics B 20, 3357.
Hammad, T. M., (2006), Material Science Forum 514-516, 1155.
Hancock, J. M., et al. (2015), Harrison,Journal of Nanoscience and Nanotechnology 15, 3809.
Hammad, T. M., (2002), Annalen Der Physik 11, 463.
Hammad, T. M. & Tamous, H. M.(2002), Chinese Journal of Physics 40, 532
Bagwe, R. P., & Khilar, K. C., (2000), Langmuir16, 1905.
Zamiri, R., Lemos, A., Reblo, A., & Ahangar, H. A., (2014), Ceram Int. 40, 523.
Qin, D., Zhang, L., He, G., & Zhang, Q., (2001), Mater Res Bull. 48, 3644.
Joo, J. et al. (2003), J Am Chem Soc. 12, 11100.

Ezenwa, I. A., Okereke, N. A., & Egwunyenga, N. J., (2012), Int J Sci Technol.2, 101.
Hwang, I. & Yong, K., (2013), Chem, , Phys Chem. 14, 364
Liu, J.C., Raveendran, P., Shervani, Z., & Ikushima, Y., (2004), Chem, Commun. 47, 2582.
Armelao, L. et al. (2002) Mater. Chem. 12, 2401
Xiao, J. P., Xie, Y., Tang, R., & Luo, W., (2002), J. Mater. Chem. 12, 1148.
Kumar, R.V., Palchik, O., Koltypin, Y., Diamant, Y., & Gedanken, A., (2002), Ultrason, Sonochem.9, 65
Chen, M., Xie Y., Chen, H. Y., Qiao, Z. P., & Qian, Y. T., (2001), J. Colloid Interface Sci. 237, 47.
Lim, W.P., Zhang, Z., Low, H. Y., & Chin, W. S., (2004), Angew. Chem. Int. Ed. 43, 5685.
Bhargava, R. N., Gallagher, D., Welker, T., & Lumin, J.,(1994), 60, 275.
Fakhri, A., Pourmand, M., Khakpour, R., & Behrouz, S., (2015), Journal of Photochemistry and Photobiology B: Biology, 149, 87.
Azam, E.S., (2014), Journal of Industrial and Engineering Chemistry 20, 4033.
Maaz, K. et al. (2007), J. Magn. Mate.308, 289.
David, G. C., Wayne, K. F., Kenneth, E. G., Gerald, D. M., & Arun, M., (2003), J. Applied Physics 93, 793.
Azam, A., Jawad A., Ahmed, A. S., Chaman, M., Naqvi A. H., (2011), J. Alloys Compd. 509, 2909.
Giribabu, G., Reddy, D. A., Murali, G., & Vijayalakshmi, R. P., (2013), AIP Conf. Proc. 1512, 186.
Hocaoglu, I. et al. (2012), J. Mater.Chem. 22, 14674.
Ovchinnikov, O. V. et al. (2015), Semiconductors 49, 373.
DK, M., XK, H., HY, Z., JH, Z., & YT, Q., (2007), J Cryst Growth, 304, 163.
Hammad, T. M., (2009), Phys. Status Solidi A 206, 2128.
Hammad, T. M., & Hejazy, N. K., (2012), International Nano Letters, 2, 2.